

Light-induced annihilation of Frenkel defects in methyammonium lead iodide perovskite

Edoardo Mosconi,^{a,b*} Daniele Meggiolaro,^b Henry Snaith,^c Samuel D. Stranks,^{d,e} * Filippo De
Angelis^{a,b}

^a Computational Laboratory for Hybrid/Organic Photovoltaics (CLHYO), CNR-ISTM, Via Elce
di Sotto 8, 06123, Perugia, Italy.

^b CompuNet, Istituto Italiano di Tecnologia, Via Morego 30, 16163 Genova, Italy.

^c Clarendon Laboratory, Parks Road, Oxford, OX1 3PU, United Kingdom.

^d Research Laboratory of Electronics, 77 Massachusetts Avenue, Cambridge, MA 02139, United
States.

^e Cavendish Laboratory, J J Thomson Ave, Cambridge, CB3 0HE, United Kingdom.

E-mail: edoardo@thch.unipg.it, sds65@cam.ac.uk

Supplementary Information

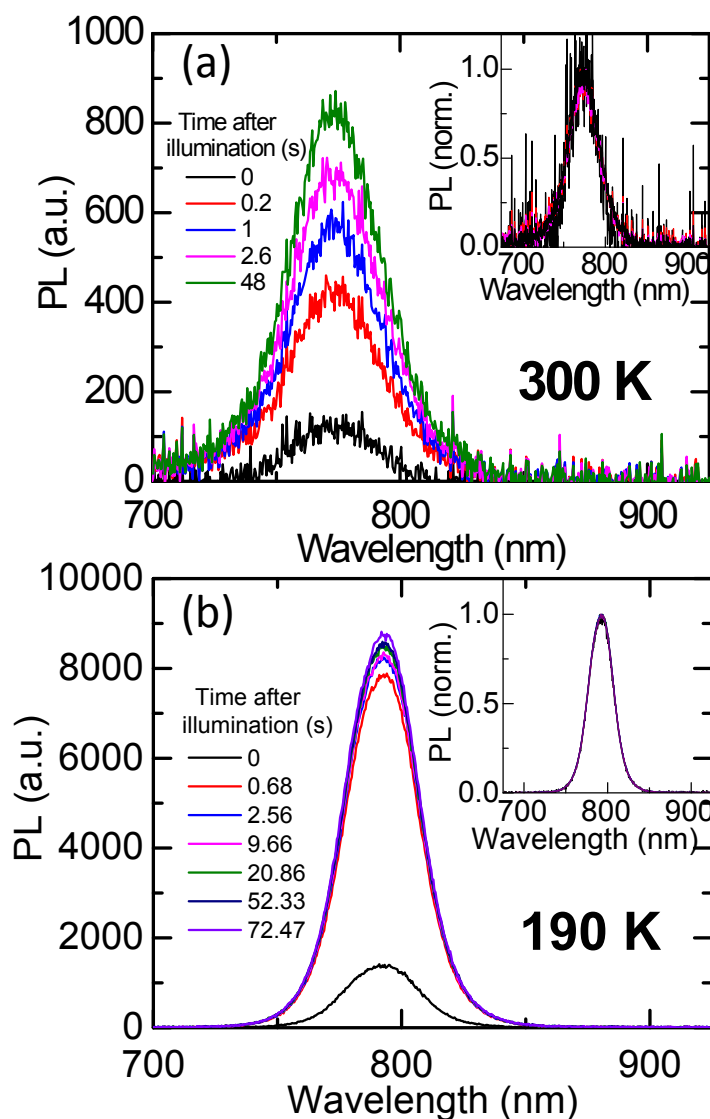


Figure S1. PL spectra at 300 K (a) and 190 K (b) from a $\text{CH}_3\text{NH}_3\text{PbI}_3$ film over time under illumination with a continuous wave (CW) laser at a wavelength of 532 nm, with an intensity of $\sim 60 \text{ mW cm}^{-2}$, producing photo-excitation densities comparable to 1-sun AM 1.5 illumination. The emission was collected using a fiber-coupled Ocean Optics Mayapro spectrometer with integration times of 20-200 ms. The insets show the normalized spectra, indicating that the PL spectral shape and position do not significantly change over time at either temperature.

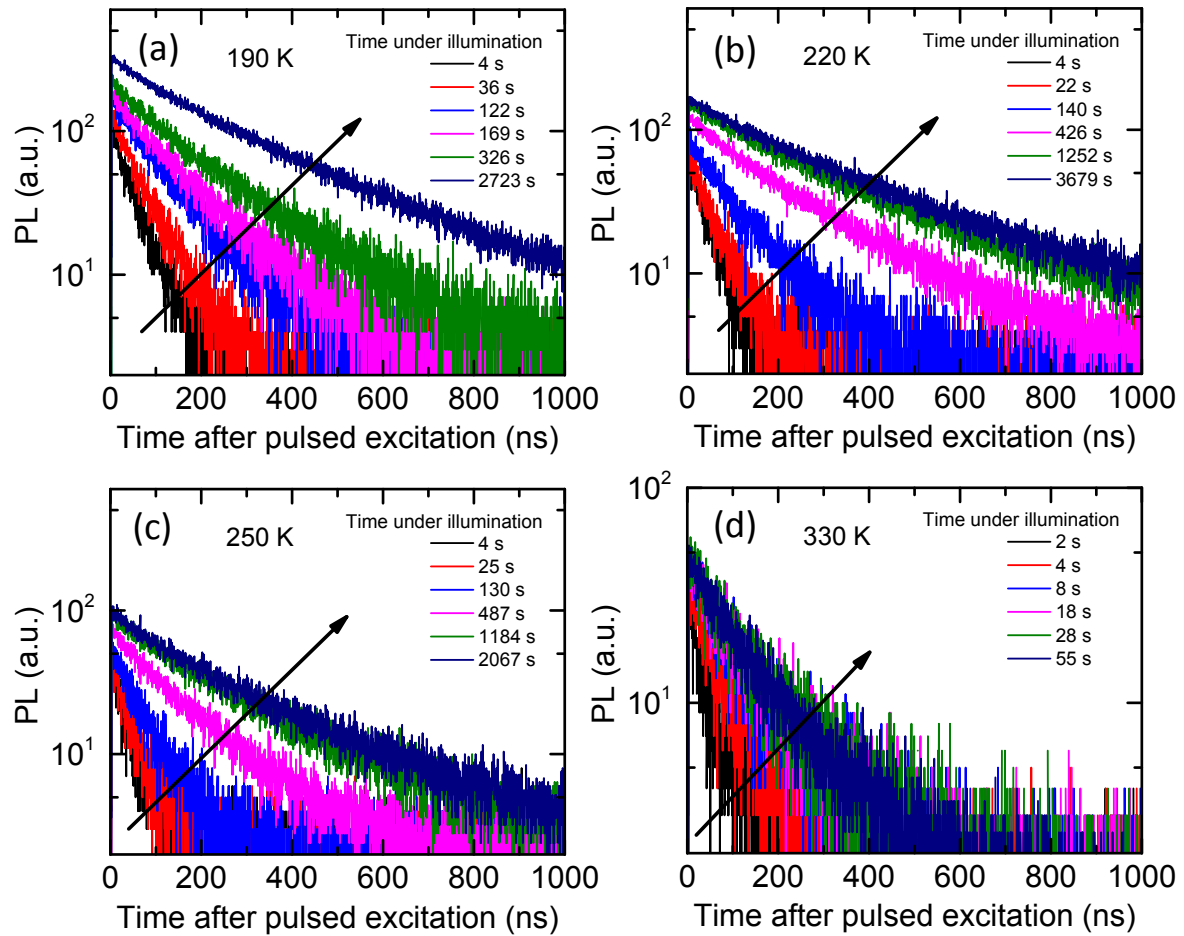


Figure S2. Temperature-dependent time-resolved PL changes over time under illumination. A selection of time-resolved PL decays from a thin $\text{CH}_3\text{NH}_3\text{PbI}_3$ film measured over time under illumination at 190 K (a), 220 K (b), 250 K (c) and 330 K (d). The stated times in the legend are time stamps at the end of the integration window for each curve. The sample was photoexcited with pulsed excitation (507 nm, 1 MHz repetition rate, 117 ps pulse length and $0.3 \mu\text{J cm}^{-2}$ per pulse) and the emission was detected at 780 nm.

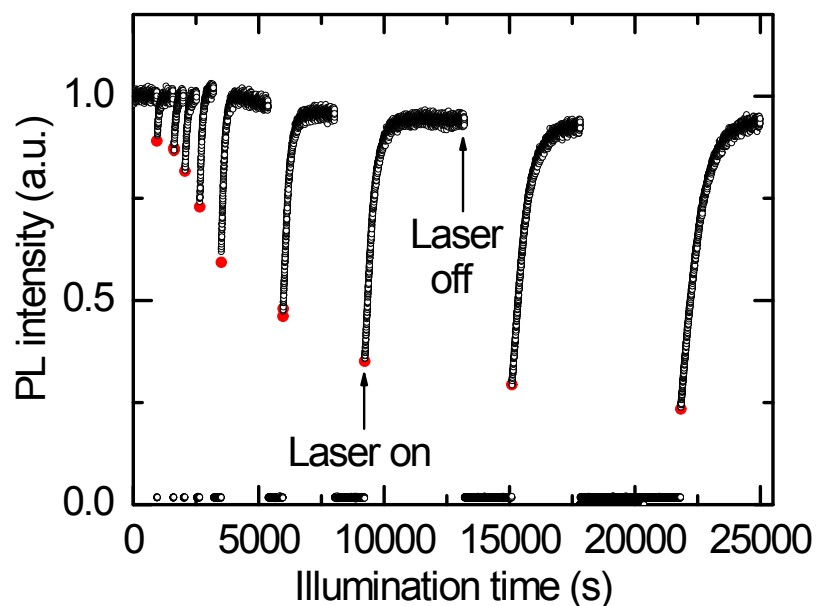


Figure S3. PL relaxation for varying times in the dark (no illumination). In each case, the PL is first allowed to reach a stabilized emission under illumination, then the laser switched off for a fixed length of time and then switched back on, with the PL continually monitored. The red closed circles represent the value of the PL intensity immediately after switching on the laser, and these values are used to generate Figure 1d. The samples were photoexcited with pulsed excitation (507 nm, 1 MHz repetition rate, 117 ps pulse length and $0.3 \mu\text{J cm}^{-2}$ per pulse) and the emission at 780 nm is time-integrated. Note the sample was first illuminated for some time to reach its initial stabilized emission level (i.e. the level at $t = 0$).

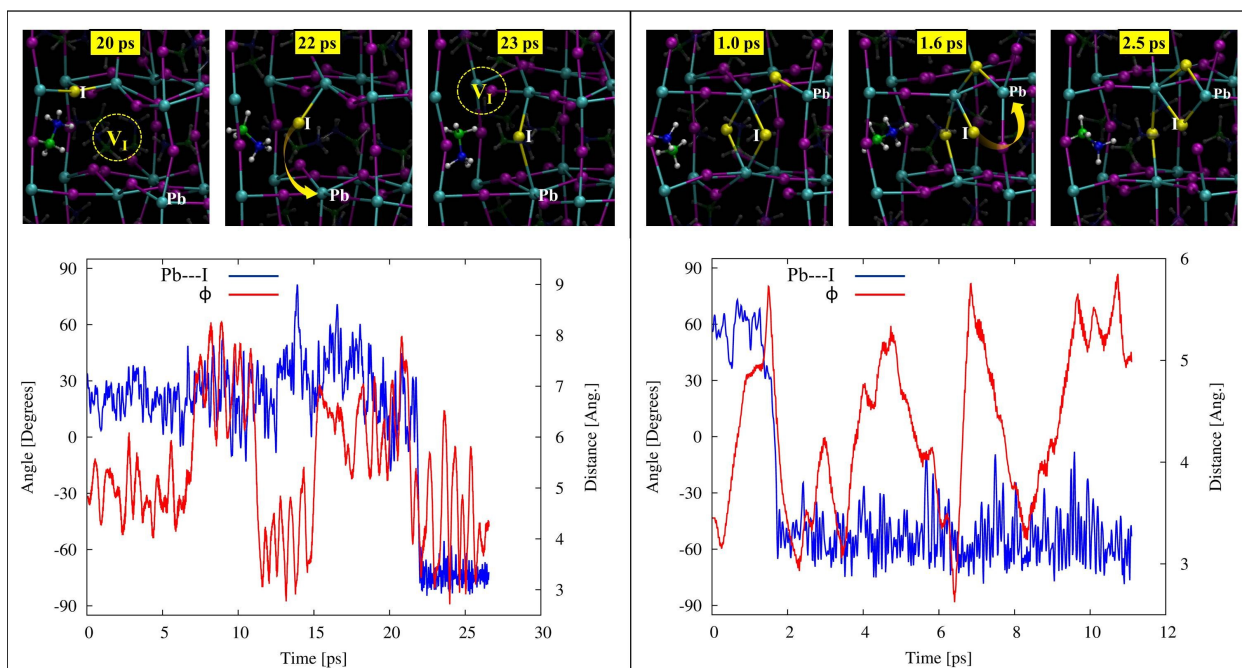


Figure S4. Dynamics of defect migration. Left (right): simulated migration of V_I^+ (I_i^-) dynamics at 450 K. The upper panels show the structural evolution characterizing the defect migration. In the lower panels we show the time evolution of selected Pb-I distances (see upper panels for atomic labels) related to migration of the defect from site to site along with the average value of the ϕ angle characterizing the global orientation of the methylammonium cations.

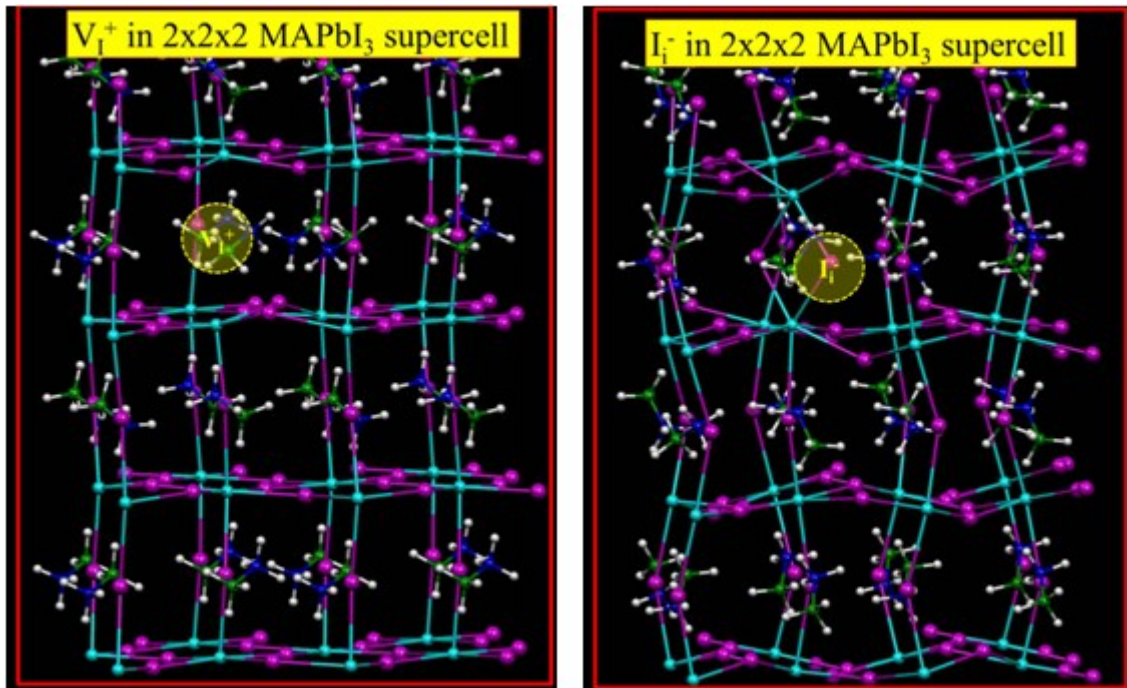


Figure S5. Supercell models for the isolated I_i^- and V_I^+ defects.

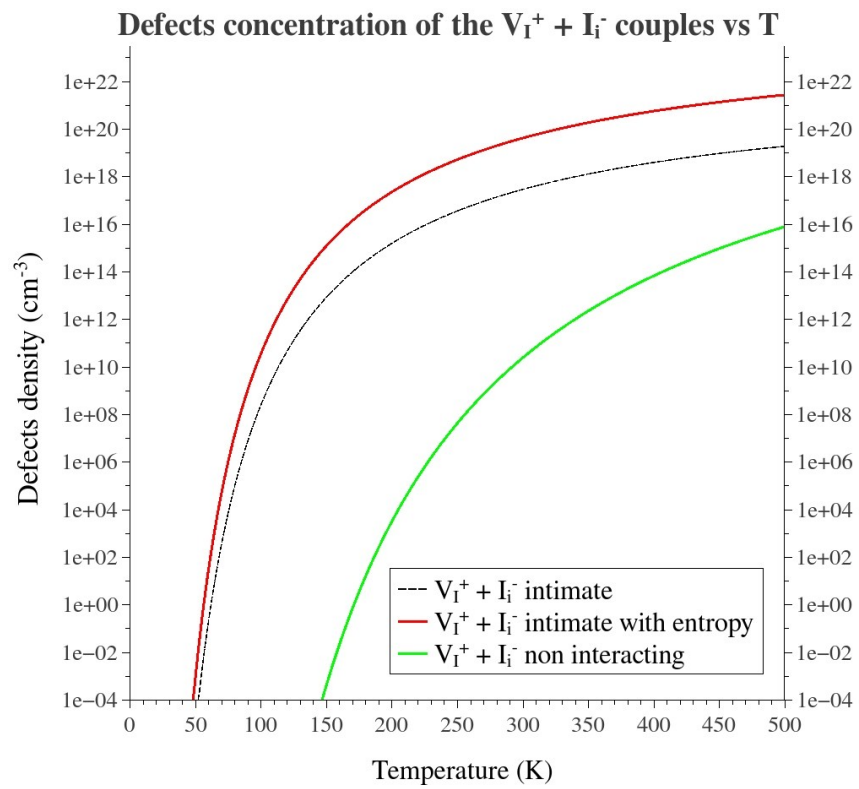


Figure S6. Density of the $V_I^+ I_i^-$ couple defects vs temperature. In black and red the density of the couple calculated at large distance in the same supercell without and with configurational entropy respectively. In green the density calculated for the isolated defects comprehensive of configurational entropy is reported.